Metalloregulatory Proteins: Metal Selectivity and Allosteric Switching

Hermes Reyes Caballero[a,b], **Gregory C. Campanello**[a], and **David P. Giedroc**[a,*]

[a]Department of Chemistry, Indiana University, Bloomington, IN 47405-7102, United States

[b]Department of Biochemistry and Biophysics, Texas A&M University, College Station, TX 77843-2128, United States

Abstract

Prokaryotic organisms have evolved an impressive capacity to quickly adapt to a changing and challenging microenvironment in which the availability of both biologically required and non-essential transition metal ions can vary dramatically. In all bacteria, a panel of metalloregulatory proteins control the expression of genes encoding membrane transporters and metal trafficking proteins, that collectively manage metal homeostasis and resistance. These "metal sensors" are specialized allosteric proteins, in which the direct binding of a specific or small number of "cognate" metal ion(s) drives a conformational change in the regulator that allosterically activates or inhibits operator DNA binding, or alternatively, distorts the promoter structure thereby converting a poor promoter to a strong one. In this review, we discuss our current understanding of the features that control metal specificity of the allosteric response in these systems, and the role that structure, thermodynamics and conformational dynamics play in mediating allosteric activation or inhibition of DNA binding.

Keywords

transition metals; metal homeostasis; allostery; repressor; energetics; protein-DNA interactions

1. Transition metal biology and metal homeostasis

Transition metals are essential to a striking diversity of biological processes in the cell. The participation of a metal ion in a specific biological process is dictated by its intrinsic properties. These range from roles as essential cofactors for oxidation-reduction reactions, electron transfer, hydrolytic and acid-base chemistry, to structural centers that merely stabilize the protein fold. Zn(II) is unique among first row transition metals in that it possesses a dual role in the cell, as both a structural element and a catalytic cofactor. For example, Zn(II) stabilizes diverse "zinc-finger" proteins that mediate binding to DNA and RNA in eukaryotes [1, 2]. On the other hand, Zn(II) is an essential cofactor of many hydrolytic enzymes, including proteases, phosphatases, esterases and deacetylases, where it functions as a Lewis acid to activate a water molecule for catalysis [3]. Other transition

*Corresponding author: Department of Chemistry, Indiana University, 212 S. Hawthorne Drive, Bloomington, IN 47405-7102, United States, giedroc@indiana.edu (D. P. Giedroc). gccampan@indiana.edu (G. C. Campanello) .

metals are cofactors in catalases and superoxide dismutases (SODs) which enables resistance to cellular oxidative stress. SODs are ubiquitous enzymes found in virtually all cells and oxygen-tolerant organisms, the importance of which is highlighted by the wide array of metal centers, from Ni to Cu to Cu/Zn to Mn and Fe, used to catalyze the same reaction, sometimes in the same cell [4]. Ni is a cofactor for urease in the stomach pathogen *H. pylori* which allows this organism to colonize the acidic gastric lumen [5].

The other side of the "double-edged sword" of transition metal biology is that essential metal ions, notably iron and copper, can undergo facile oxidation-reduction and as a result, can catalyze the production of highly toxic reactive oxygen species by Fenton or Haber-Weiss chemistry from partially reduced forms of oxygen that form as by-products of aerobic respiration [6, 7]. In addition, heavy metals and metalloids that play no biological role, including mercury, cadmium, arsenic, lead and tin, are extremely toxic often as a result of forming strong coordinate covalent bonds with cellular thiols, or calcium-binding proteins in the case of Pb(II) [8-10]. Therefore, in order to utilize essential transition metal ions while detoxifying or effluxing nonessential ones, microorganisms and all cells have evolved mechanisms to regulate the intracellular metal concentration.

The remarkably precise control of cytoplasmic metal ion concentrations is termed **metal homeostasis**, in which metallochaperones, metal importers, and metal effluxing transporters each play vital roles in regulating metal bioavailability. The expression of genes encoding these proteins is controlled by a panel of specialized transcriptional regulators known as metalloregulatory proteins, or "metal sensor" proteins (see **Section 2**). These transcriptional regulators specifically sense one or a small number of metal ions and are classified into at least ten families on the basis of structural homology [11, 12]. Binding of the cognate metal to the metalloregulator activates or inhibits protein-DNA operator binding, which results in the transcriptional regulation of genes responsible for metal homeostasis [13, 14]. In addition to encoding proteins that traffic metal ions within or between cellular compartments, the regulon may also include genes that encode proteins with functionalities beyond metal homeostasis, including virulence determinants, an oxidative or nitrosative stress response, or precursors of enzymatic pathways [15-17]. Indeed, these operons are often vital for the survival of pathogenic bacteria in humans.

An increased level of complexity is introduced when metalloregulatory networks specific for one metal ion intersect with others in the cell. Structurally unrelated metallosensors with distinct metal specificities may interact within the same cytoplasm. For example, Ni(II) and Fe(II) metalloregulators NikR and FurR in *H. pylori* have overlapping DNA binding sites in the promoter regions of their regulons [18, 19], a finding consistent with numerous examples of Ni-Fe cross-talk in cells [20, 21]. In *B. japonicum* the Fur-family regulator Irr appears to be targeted for proteolytic degradation upon heme binding. Under conditions of low iron, heme is scarce and not sufficient to signal Irr for degradation; in addition, Mn(II) binds to Irr and further stabilizes it against denaturation. Therefore, when *B. japonicum* is grown under Mn(II) depleted conditions, Irr senses heme-Fe(II) at correspondingly lower concentrations, consistent with the hypothesis that Mn(II) and Fe(II) homeostasis are interconnected [22]. Non-cognate metal binding affects transition metal homeostasis as well. For example, in the human pathogen *S. pneumoniae*, Zn(II) stress induces a strong Mn(II) deprivation phenotype, thought to be caused by competition between Zn(II) and Mn(II) at the high affinity Mn(II) uptake system and possibly in the cytoplasmic Mn(II) sensor PsaR [23, 24].

Emerging evidence reveals that transition metal homeostasis influences many fundamental aspects of bacterial cell physiology and bacterial pathogenesis [25-27], and is therefore essential to understand the metal specificity and mechanisms of metalloregulation operative within the cell [11]. Important insights into what governs these processes come from

biophysical and structural studies of purified metalloregulatory proteins. Herein, we review recent progress on two major regulatory aspects of bacterial metal homeostasis derived from physicochemical studies: 1) the coordination chemistry of metal coordination that governs the specificity of the response, and 2) structural, thermodynamic and dynamical mechanisms of allosteric regulation of operator-promoter binding by cognate vs. non-cognate metal ions.

2. Metal binding affinities of metal sensor proteins and control of metal homeostasis

Cellular homeostasis of total transition metal concentration is set within boundaries beyond which the cell experiences excess or deprivation, thereby inducing a cellular response. All cells actively concentrate cell-associated metal ions, to a degree that is more similar than different between cells, with total measurable zinc and iron in the 10^{-4}-10^{-3} M range, manganese and copper approximately 10-fold lower, with nickel and cobalt another 10-fold lower [24, 28]. In prokaryotes, the cellular response to perturbations in metal homeostasis is nearly exclusively transcriptional. In many cases, a promoter exclusion model is operative where a transcriptional repressor binds to a specific DNA operator which sterically blocks the binding of RNA polymerase [29, 30]. A significant departure from this model is transcriptional activation by MerR-family regulators, where the metal-bound or otherwise "activated" form of the repressor allosterically changes the structure of the promoter from a poor promoter to a strong promoter, without protein dissociation [31-33].

In the former case, the simplest mechanism of allosteric regulation of operator binding requires that a metalloregulator (P) has at least one DNA binding site or domain (D) and one metal (M) regulatory site, often but not always located in structurally separated domains within a homooligomer (dimer or tetramer). The "ligand" binding sites can interact with each other in two distinct ways: If the binding of M stimulates the binding of D then this is termed positive allosteric regulation, and occurs most often in metal-mediated repression of uptake genes. On the contrary, if the binding of M antagonizes the binding of D, this manifests as negative heterotropic allosteric regulation, and it is this process that occurs most often in metal-mediated transcriptional derepression [12] (Fig. 1).

When the cytoplasm is experiencing metal excess, derepression of genes encoding for metal efflux or detoxification proteins, and concomitant repression of genes encoding metal uptake systems, will restore the cytoplasm to homeostasis. Thus, a long-standing hypothesis is that the intracellular metal *activity* or *free metal* concentration at which a metalloregulator is inhibited or activated to bind to its operator (or allosterically change the promoter structure) establishes the threshold or sensitivity of the transcriptional response [28]. This hypothesis holds that the reciprocal of the metal association equilibrium or metal affinity constant K_{Me}, ($1/K_{Me}$), defines the buffered or labile pool of metal at half-maximal activation or inhibition of the transcriptional response (Fig. 2).

To help illustrate this point, zinc homeostasis in *E. coli* is controlled by two metalloregulatory proteins, Zur and ZntR (Fig. 2). The Zn(II) sensor Zur is a member of the Fur family [34] that represses the expression of *znuABC*, which encodes a Zn(II) uptake ABC transporter in the presence of Zn(II). Conversely, ZntR is a MerR regulator that activates the transcription of *zntA*, a gene encoding a P-type ATPase that effluxes zinc from the cytoplasm to the periplasm [32, 35]. *In vitro* transcription experiments reveal that each metalloregulator competes for Zn(II) with an affinity constant ($1/K_{Me}$) offset by approximately one log unit, resulting in an activation threshold positioned at approximately femtomolar (10^{-15} M) Zn(II) [28]. As shown in Table 1, other Zn(II) metalloregulatory proteins bind Zn(II) with log K_{Me} of ≈12-13 at or above neutral pH; if this hypothesis is correct, then Zn(II) may well be buffered at somewhat higher concentration, 10^{-12}-10^{-13} M

in other microorganisms. In the eukaryotic cell, cytosolic Zn(II) is buffered at $\approx 10^{-9}$ M, with a labile pool of 0.2 μM in the mitochondrial matrix [36]. This suggests that the bacterial cytoplasm and mammalian cytosol possess different buffering capacities for zinc.

The Irving-Williams series of divalent metals ions establishes that Zn(II) and Cu(II) bind with the highest affinity to a model chelate, while Mn(II) and Fe(II) bind with the lowest affinity to the same chelate, Zn≤Cu>>Ni≥Co≥Fe≥Mn [11, 37]. Metalloregulatory proteins that have been extensively characterized largely follow this expected trend, although there are also some outliers (Table 1). The Irving-Williams series classifies Zn(II) as a highly "competitive" metal, *i.e.,* Zn may be capable of binding as a non-cognate metal far more tightly than the corresponding cognate metal (K_{Zn}>>K_{Mn} for *B. subtilis* MntR, for example) (Table 1). As a result, the cytoplasm employs an overcapacity to chelate Zn(II), and it has been postulated that ribosomal proteins play an important role in this process [38-40]. The obligatory participation of specific metallochaperones that traffic Cu(I) to target proteins with $K_{Cu(I)}$≥10^{18} M^{-1} also likely reflects the need to maintain the bioavailable concentration of this metal under very tight control as well [41, 42]. As a result, *E. coli* CueR, a copper-selective member of the MerR family, is activated by Cu(I) *in vivo* and binds Cu(I) with an affinity of $10^{20.7}$ M^{-1} [43] (Table 1). Other copper sensors, *e.g.* CsoR, are characterized by a log $K_{Cu(I)}$ of 18-19, in range of that of CueR [44-46]. Thus, this hypothesis suggests that Zn(II) and Cu(I) are buffered in cytoplasm in the picomolar-femtomolar and attomolar-zeptomolar range, respectively (Fig. 2). In contrast, *E. coli* Fur, an Fe(II)-dependent transcriptional repressor responds to the low micromolar range of iron (Table 1) [47], with binding affinities for Mn(II) regulators in the 10^3-10^5 M^{-1} range of K_{Me} (Table 1). These affinity constants suggest that a correspondingly larger fraction of the Mn(II) and Fe(II) concentrations in the cell may be weakly bound or highly mobile with rapid off-rates [13] (Fig. 2).

The degree to which pairs of metalloregulators possess relatively well-matched metal affinities and specificities is not yet known. For example, a Cu(I) uptake regulator or an Fe or Mn efflux regulator have not yet been identified which suggests that "one-armed" transcriptional control (see Fig. 2) may be sufficient to maintain intracellular homeostasis of Cu(I) and Fe/Mn. The case of Ni(II) homeostasis in *E. coli* provides an interesting contrast to these systems. Like Zn(II), Ni(II) homeostasis in *E. coli* is controlled by a pair of regulators, in this case NikR and RcnR. NikR is a Ni(II)-specific D_2-symmetric homotetrameric repressor [48, 49] that controls the transcription of *nikABCD*, a high affinity Ni(II) uptake transporter [50, 51]. NikR binds Ni(II) to the each C-terminal regulatory site at the tetrameric interface with affinity of 10^{12} M^{-1} [49, 52]. RcnR is a Ni(II) specific efflux regulator from the CsoR family that dissociates from the DNA operator sequence when Ni(II) binds, allowing the expression of *rcnA,* a gene that encodes for a Ni(II)/Co(II) transporter [53]. Ni(II) binds to RcnR with an affinity of $\approx 10^{7.6}$ M^{-1} or approximately five orders of magnitude weaker than NikR at a similar pH (Table 1). Thus, NikR and RcnR possess poorly matched Ni(II) affinities and thus would appear to be in contrast to the zinc sensor pair in *E. coli* [54] (Fig. 2). However, NikR is known to possess an additional pair of low affinity Ni(II) regulatory sites (log K_{Ni}= 9) that are required for full NikR repression [55, 56]. This might suggest an ordered or step-wise regulatory response in the cell where uptake is first partially repressed, and then fully repressed, prior to Ni(II) efflux re-establishing Ni(II) homeostasis. Interestingly, two paralogous efflux regulators from the ArsR family [57] present in *M. tuberculosis*, NmtR and KmtR, may well collaborate to establish a similar two-step or graded repression response to Ni(II) toxicity as well, given log K_{Ni} values of 12 and 10, respectively [29, 58] (H. Reyes-Caballero and D. Giedroc, manuscript in preparation). The physiological importance of a potentially graded response to nickel toxicity in *E. coli* and *M. tuberculosis* has not yet been firmly established. The recent discovery of a two pairs of metalloregulatory sites within homodimeric *S. coelicolor* Zur

[59], which appear to influence zinc-mediated repression at different promoters to different degrees, is also consistent with a graded response to zinc stress in that organism as well [60]. The sensitivity of the zinc efflux regulator has not yet been established in *S. coelicolor*.

Ongoing studies in our laboratory are focused on the control of Zn(II) homeostasis in *S. pneumoniae*, where two metal sensor proteins, AdcR and SczA, function to control the expression of genes that encode for Zn(II) uptake and efflux, respectively. AdcR is the first known metal-sensing MarR family member [61], and binds Zn(II) with an affinity of 10^{12} M^{-1} at pH 8.0 [15] as would be anticipated on the basis of K_{Zn} found for other Zn(II) metallosensors (Table 1). However, preliminary findings with SczA, a novel Zn(II) sensing TetR family member [62] reveals K of $\approx 10^8$ M^{-1} Zn under the same conditions (K. Geiger and D. Giedroc, unpublished results), or about four orders of magnitude weaker than K_{Zn} for AdcR. This is consistent with expression analysis which suggests that under all conditions containing ≥20 μM total zinc in liquid media, the AdcR regulon is fully repressed and the cellular response to perturbation of zinc homeostasis is governed exclusively by SczA and metal efflux [15, 24].

3. Metal selectivity, ligand donor sets and coordination geometry

A large number of metal sensor proteins have now been structurally characterized by x-ray crystallography, NMR spectroscopy and other spectroscopic methods. As a result, it is now possible to identify common features of metal sensing sites specific for a particular metal ion (Fig. 3). Transition metal ions become more polarizable or "soft" as the number of *d* orbital electrons increases. Although the first row transition metal ions Fe(II), Co(II), Ni(II), Cu(II) and Zn(II) are considered as a group to be borderline hard/soft, subtle ligand preferences are apparent as Mn(II) is *d*5 and is considered "hard" relative to *d*10 Zn(II) which is correspondingly "soft". Likewise, Cu(I) is more polarizable than Cu(II) since a decrease in valence means an additional *d*-electron has been added. Soft metals prefer soft ligands, with the trend in polarizability decreasing from Cys to His/Met to Asp/Glu.

These trends in metal-ligand polarizabilities from small molecule coordination chemistry are largely recapitulated in metal ligand donor sets in metal sensor proteins. This has been most extensively established in the ArsR/SmtB (or ArsR) family of metalloregulatory proteins, widely represented across bacterial species [14, 57, 58]. ArsR family proteins regulate the expression of genes that encode for proteins responsible for metal ion detoxification, sequestration and cytoplasmic efflux, as well as many other processes not yet discovered [58]. The metalloregulators of this family have collectively evolved an impressive range of regulatory metal binding sites on a relatively unchanging protein scaffold with clearly distinct metal specificities [12]. Soft metal ion sensors from the ArsR family, such as Cd(II)/Pb(II) sensor *S. aureus* CadC, the Cd(II)/Pb(II) sensor *M. tuberculosis* CmtR, As(III)/Sb(III) sensor *E. coli* ArsR, and Cu(I) sensor *O. brevis* BxmR, all harbor metal regulatory sites that are rich in cysteine residues. In contrast, the Zn(II)/Co(II) sensor *S. aureus* CzrA [63] and the Ni(II)/Co(II) *M. tuberculosis* sensor NmtR bind the metal with more electronegative and less polarizable "hard" donor ligands including glutamate and aspartate residues (Fig. 3).

B. subtilis MntR is a Mn(II)-dependent repressor of the transcription of *mntABCD* which encodes a high affinity Mn(II) importer. MntR binds Mn(II) weakly with K_{Mn} in the order of 10^5 M^{-1} [64] (Table 1), yet is Mn(II)-specific among first-row transition metal ions *in vivo* [65]. Structurally MntR is similar to the Fe(II) sensor DtxR/IdeR [66, 67], but is a stable dimer that binds one to two metal ions per subunit depending on solution conditions [68]. Among non-cognate metals, Cd(II) activates MntR *in vitro* to the same or greater degree while Zn(II), Ni(II), Fe(II), and Cu(II), activate DNA binding with low efficacy [69]. A similar metal specificity profile characterizes DtxR-like family repressors PsaR and ScaR

from *Streptococcus spp.* [24, 70]. Selective allosteric switching by Mn(II) over Fe(II) appears to be largely based on ligand preferences of Mn(II) vs. Fe(II) [71]. The metal regulatory sites in MntR and DtxR/IdeR are structurally equivalent yet differ in the nature of the coordinating ligands. Here, the thioether sulfur of Met10 in the α1 helix and thiolate sulfur of Cys102 in the regulatory domain found in the Fe(II) selective repressor DtxR/IdeR are replaced by Asp8 and Glu99, respectively, in Mn(II)-specific MntR [71]. Inspection of the structural database confirms that nature selects against coordination of Mn(II) by cysteine [72] in contrast to the well known propensity of Fe(II) to form iron-sulfur clusters of varying nuclearities [71]. On the other hand, Mn(II) selects against Zn(II) on the basis of distinct coordination geometries of each, since the tetrahedral coordination of Zn(II) differs from the native more highly coordinated hexa- or heptavalent coordination geometry observed for Mn(II) and Cd(II), respectively [64, 73].

The *S. aureus* Zn(II) metalloregulator CzrA of the ArsR family represses the transcription of the cation diffusion facilitator (CDF) CzrB in the absence of metal stress [14]. CzrA is denoted an "α5" ArsR family sensor as it binds Zn(II) with negative homotropic cooperativity at two regulatory sites positioned between the pair of α5 helices at the dimer interface with step-wise binding affinities K_{Zn1} and K_{Zn2} of $\approx 10^{12}$ M^{-1} and $\approx 10^{10}$ M^{-1}, respectively, at pH 7.0 (Table 1) [63, 74]. Functional characterization of metal ligands in the α5 helix shows a tolerance for variation at some liganding positions, while other metal ligands are absolutely essential for allosteric regulation of DNA binding [63]. In contrast, the mutagenesis of any of the α5 ligands in the homologous Ni(II)/Co(II) sensor *M. tuberculosis* NmtR abrogates allosteric inhibition of DNA binding (H. Reyes-Caballero and D. Giedroc, manuscript in preparation). NmtR binds Ni(II) in an octahedral coordination geometry, but shares an analogous core of four α5 ligands with CzrA [75].

Comparative structural and spectroscopic studies of CzrA and the related zinc sensor, *Synechococcus* SmtB with NmtR reveals a key aspect of regulation by "α5" ArsR family sensors. These studies establish that Zn(II) binds in a tetrahedral or distorted tetrahedral coordination geometry to CzrA and SmtB [63, 76] while Ni(II) binds to NmtR in an octahedral coordination geometry [75]. These coordination geometries parallel the natural preferences of each metal [77-80]. However, a non-cognate metal ion will often bind to the same site in such a way to force a new non-native coordination geometry, consistent with intrinsic preferences of the non-cognate metal [75]. However, formation of a non-native coordination geometry always results in a weaker or abrogated allosteric response, relative to the cognate metal, and thus a poorer ability to sense these metals in the cell. For example, in the functional analysis of the α5 metal ligand chelate of CzrA, only those substitutions that preserved a native tetrahedral Zn(II) coordination geometry were capable of allosteric regulation of DNA binding *in vitro* and could adopt an allosterically inhibited conformational state, irrespective of K_{Zn} [63]. These findings on CzrA support the hypothesis that the structure of the first coordination shell around the cognate metal is a major determinant of biological specificity [63].

Detailed studies with other regulators are largely consistent with this hypothesis. The *M. tuberculosis* Cu(I) dependent repressor, $CsoR_{MT}$ is a founding member of a large family of bacterial regulatory proteins [46, 54, 81]. *M. tuberculosis* CsoR controls the expression of *ctpV,* a gene that encodes a predicted copper ATPase that effluxes Cu(I) from the cytoplasm [81]. CsoR binds to Cu(I) with an association equilibrium constant in the order of 10^{18} M^{-1} [44, 45]. CsoRs from *Bacillus subtilis* ($CsoR_{BS}$) and *S. aureus* ($CsoR_{SA}$) are homologous to $CsoR_{MT}$ and each adopts a S_2N coordination complex that is structurally identical to that of $CsoR_{MT}$ [45, 46] (Fig. 3). $CsoR_{BS}$ also binds Zn(II) and Ni(II) tightly in what appear to be non-native tetrahedral and square planar geometries, respectively, but these metals are quantitatively less capable than trigonal Cu(I) of driving dissociation of $CsoR_{BS}$ from the

DNA operator [45]. In contrast, the CsoR-family Ni(II) efflux regulator *E. coli* RcnR [12] adopts an octahedral coordination geometry upon binding cognate metals Ni(II) and Co(II) by recruiting additional metal ligands from the N-terminal region that are not found in the copper sensor CsoR; this results in an $S(N/O)_5$ coordination sphere [54]. The metal specificity of CsoR and RcnR for Cu(I) or Ni(II) is therefore dictated by the coordination geometry which may or may not track with metal affinity [82], analogous to the conclusions reached with the ArsR family of regulators.

Full repression by the Ni(II) sensor *E. coli* NikR is also observed *in vivo* only when cognate metal Ni(II) binds in a square planar coordination geometry to the C-terminal regulatory sites. Cu(II) forms a complex that is isostructural with that of Ni(II), but will not be regulatory *in vivo* due to the vanishingly small concentrations of Cu(II) expected to be present in the reducing bacterial cytoplasm (see Fig. 2) [54]. However, a clearly non-native coordination geometry is adopted by all other non-repressing metals; Zn(II) adopts a tetrahedral coordination geometry and Co(II) an octahedral complex. As expected, both metals poorly activate DNA operator binding by NikR [50, 55, 83, 84].

This close correspondence of functional metal selectivity and coordination geometry also characterizes other classes of metalloregulatory proteins, including the transcriptional activators of the MerR family from *E. coli*, CueR and ZntR. In MerR family proteins, metal ions typically bind to a C-terminal loop which is packed against the N-terminal DNA binding domain. CueR binds Cu(I) in a characteristic linear Cu(I) *bis*-thiolato coordination geometry [85], a coordination structure also observed for CueR in complex with Ag(I) and Au(I) [43] (Fig. 3). In contrast, Zn(II) binds to ZntR to form a phosphate-bridged binuclear Zn(II) center, with each Zn(II) ion adopting a tetrahedral coordination geometry [43] (Fig. 3). Finally, the Fur family Ni(II) sensor Nur [86] has been proposed to discriminate against other metals by harboring an octahedral coordination site not found in other Fur family repressors, with an additional site analogous to the regulatory Fe(II) binding sites in the Fe(II)-specific regulator, Fur [87]. In contrast, the regulatory site(s) in the Zn(II)-specific Fur family regulator, Zur, clearly adopt four-coordinate tetrahedral complexes [60, 88], fully consistent with nearly all other Zn(II) regulators, with the exception of AdcR [15]. In no case, however, have systematic quantitative studies been carried out to assess the degree to which the coordination geometry of the cognate or regulatory metal differs from that of a non-cognate metal in allosteric activation of DNA binding.

4. Allosteric signal propagation

The studies summarized above establish that the structure of the first coordination shell adopted by cognate vs. non-cognate metal ions is a major determinant for biological metal specificity. Recent structural studies are beginning to reveal *how* formation of a native coordination geometry is tied to structural changes in a repressor [89, 90]. Early crystallographic structures of the apo- and Zn(II) forms of *Synechoccocus* SmtB and *S. aureus* CzrA provided the first insights into a possible structural coupling mechanism [91]. Two hydrogen bonds appeared to form a pathway that connected the α5 metal center and the α4 DNA recognition helix on the opposite protomer through the αR'-β1 loop upon metal binding (Fig. 4). The non-chelating nitrogen (Nε2) of the essential ligand His117 (H97 in CzrA) forms a key second coordination shell hydrogen bond and is therefore predicted to be responsible for triggering the allosteric response upon Zn(II) binding [91]. Support for this model came from the observation of an intense Nε2-Hε2 correlation from His117 in the ^1H-^{15}N HSQC spectrum, which is lost upon metal dissociation [91] (Fig. 4). Analogous observations are found for His97 in the related Zn(II) sensor CzrA [91, 92] (Fig. 4).

Semisynthetic native chemical ligation is currently being used to directly test this allosteric coupling model in CzrA by site-specifically incorporating unnatural His97 analogs designed to maintain an Nδ1-Zn(II) coordination bond, but lack the ability to donate a hydrogen bond on the other side of the imidazole ring (Z. Ma., Y. Fu and D. Giedroc, manuscript in preparation) (see Fig. 4(b)). Such an approach was recently employed on the Cu(I) sensor *M. tuberculosis* CsoR in which it was established that the nonliganding Nε2 face of His61 mediates a hydrogen bonding network to Tyr35′ and Glu81 across the subunit interface to stabilize the low DNA binding affinity of the tetramer [44]. Although the precise structural mechanism of Cu(I) regulation in CsoR is not completely understood, these second coordination shell interactions seem to be required for allosterically coupling cognate metal binding and DNA binding sites. The neutral charge of the histidine side chain at physiological pH and the frequency of events of this kind found in structural databases [93, 94] reveal that nature exploits a recurring mechanism to enable allosteric signal propagation in metal sensor proteins. Current efforts are underway to identify other allosteric residues in CzrA.

The mechanism of activation of DNA binding by Fur family transcriptional repressors is based largely on studies of the hydrogen peroxide sensor PerR, which employs an iron chelate to sense oxidative stress in *B. subtilis*. Here, the metal ligand His37 from the N-terminal winged helix DNA binding domain effectively couples the N-terminal and C-terminal domain which stabilizes a "closed" Fe(II)- bound conformation that activates binding of PerR to operator sites upstream of oxidative stress sensing genes (Fig. 4) [95]. Mechanistically, PerR uses an open coordination site on Fe(II) to bind H_2O_2, which results in oxidation of Fe(II) to Fe(III) and creating OH• which in turn leads to oxidation of two metal liganding histidines, His37 and His91, to 2-oxo-histidine [96]. This is thought to lower the affinity of PerR for Fe(III), allowing for metal dissociation, and triggering a quaternary structural change leading to an "open" apo-like structure of lower DNA binding affinity, as predicted by the crystal structure of inactivated (apo) PerR (Fig. 5) [95, 97, 98]. All ligands in the regulatory site are essential for peroxide sensing *in vivo*, but each plays a distinct function. His37 appears to function in a key allosteric role, but this time via ligand oxidation and perturbation of the *first* coordination shell; this effectively uncouples the DNA binding domain from the regulatory domain. His91, on the other hand, is predicted to play an important role in stabilizing the Fe(II) complex; oxidation therefore simply increases dissociation of the metal, which drives "open" the molecule [99, 100] (Fig. 5).

Other Fur family repressors bind metal ions to activate DNA binding to Fur-boxes upstream of genes that often encode for metal ion uptake systems [101]. In the available structures of Fur homologs that are activated to bind DNA by divalent metal ions, *e.g.*. zinc-sensing *M. tuberculosis and S. coelicolor* Zur [60, 88, 102], *P. aeuroginosa*, *V. colera* and *H. pylori* Fe(II) sensors Fur [72, 103, 104] and the Ni(II) sensor *Streptomyces coelicolor* Nur [86], all possess metal binding sites that are structurally analogous to the Fe(II) site in PerR. In most of these cases, it has been hypothesized that coordination of metal ions anchored by a conserved pair of His residues analogous to His37 and His91 in *B. subtilis* PerR stabilizes a "closed" conformation that is competent to bind operator DNA [72, 95] (Fig. 5).

5. Thermodynamics of allosteric regulation by metals

An emerging topic in the study of allosteric regulation in metal sensor proteins is the measurement of the energetics and conformational dynamics that underlie the mechanism of metal activation or inhibition of DNA operator binding. These studies are motivated in part by a lack of a dramatic structural change observed when comparing the metal-bound vs. metal-free crystal structures of ArsR/SmtB sensors, for example [91]. This picture differs dramatically from the large conformational change in PerR and perhaps other Fur family

regulators as well as in NikR [90] discussed above (see Fig. 5). In MerR family activators, there is little understanding of this process due to incomplete structural characterization of all relevant allosteric states, *e.g.,* apo-, ligand-bound, DNA-bound ligand activated, within a single MerR regulator [33, 105] Indeed, accumulating evidence suggests that allosteric proteins can clearly function in the absence of large structural changes, mediated instead by changes in conformational dynamics, *e.g.,* stiffening or enhanced mobility, that can be detected by residue-specific NMR methods (see Section 5) or globally through thermodynamic methods [106-108].

Although biological systems are open systems that operate far from equilibrium [109], the study of metalloregulatory proteins in equilibrium with its two ligands, DNA operator and metal ion, represents a powerful tool that has enabled the discovery of many fundamental aspects of metalloregulation [13, 74]. This coupled equilibrium can be cast in terms of a simple thermodynamic cycle (Fig. 1; Fig. 6) [13]. The magnitude of the thermodynamic linkage, ΔG^t_C, defines the efficacy of the allosteric ligand (metal) to activate or inhibit DNA operator binding. Such a formalism facilitates quantitative comparisons of different metal sensor proteins with different metal ions, but more importantly provides a thermodynamic construct with which to identify key residues that are involved in the allosteric switching mechanism, independent of their effect on binding affinity for either ligand [13, 44, 110].

Isothermal titration calorimetry (ITC) has recently been used to measure a complete set of thermodynamic parameters for the binding of Zn(II) to CzrA homodimer in the free form and in the protein-DNA complex. This approach has allowed extraction of the homotropic coupling free energies within the two states and ultimately the step-wise heterotropic coupling free energies, ΔG_c^i (Fig. 6) [74]. The Zn(II) binding isotherms were readily fit to a two-step binding model where the energetics associated with formation of the Zn_1-CzrA and Zn_2-CzrA complexes could be measured in the free and the DNA bound complex (*top, bottom* horizontal equilibria, Fig. 6). The first Zn(II) binding event to the apoprotein is entropically driven ($-T\Delta S_1 = -16.6$ kcal mol^{-1}), with a small opposing enthalpy term ($\Delta H_1 = 0.06$ kcal mol^{-1}) [74]. Structurally, this Zn_1 state is characterized by a loss of symmetry detectable in an ^{1}H-^{15}N HSQC spectrum, representing a superposition of apo and metallated states, consistent with strong negative cooperativity of metal binding [63, 111]. The magnitude of the heat capacity change ($\Delta C_p^1 \approx -230$ cal mol K^{-1}) may be reporting on solvent reorganization as a result of restructuring the dimer interface [74]. In striking contrast, binding of the second Zn(II) to Zn_1-CzrA is entropically less favorable by ≈ 5 kcal mol^{-1} ($-T\Delta S_2 = -11.9$ kcal mol^{-1}) relative to the first binding event (Fig. 6). This is thought to be the energetic origin of negative homotropic cooperativity of Zn(II) binding, where the second site globally quenches the short timescale dynamics [74].

These thermodynamics of Zn(II) binding contrast sharply with those obtained with the repressing apo-CzrA-DNA complex. Here, the entropic penalty for the binding of the second Zn(II) relative to the first is far smaller ($\Delta(-T\Delta S)'=0.6$ kcal mol^{-1}) suggesting that the Zn_2-CzrA-DNA complex is far more dynamic than unbound Zn_2 CzrA [74]. Parallel differences are observed in the sign and magnitude of the enthalpy term, which while overall favorable in the unbound state, is unfavorable or near zero ($\Delta H_2' - \Delta H_1' \approx 0.7$ kcal mol^{-1}) in the DNA complex; this is consistent with the greatly reduced $\Delta(-T\Delta S')$. Thus, although metal binding to the protein-DNA complex is also negatively cooperative ($\Delta\Delta G=1.3$ kcal mol^{-1}), the underlying energetics are completely different. This in turn drives strong negative allosteric (heterotropic) cooperativity in this system, ΔG_c^t, which is sizable at 6.3 kcal mol^{-1}. In experiments that employed a covalently fused CzrA dimer, the intermediate Zn_1-CzrA state shows metal dependent inhibition of DNA binding *in vitro* to 70% of the fully metallated Zn_2-state [111]. In contrast, the stepwise coupling free energies, ΔGc^1, ΔGc^2, were found to make approximately equal contributions to ΔG_c^t [74] (Fig. 6). The origin of

this discrepancy is unknown but it may lie in the covalent coupling of the C-terminus of one protomer to the N-terminus of the other, since the linker length was found to have a profound influence on the stoichiometry and cooperativity of Zn(II) binding to various fused CzrAs [111].

It is interesting to note that studies like these have the potential to systematically access all four allosteric "end-states," including the ternary CzrA-Zn$_2$-DNA complex (P•Me$_2$•D in Fig. 1) [112]. This complex is likely a transiently formed intermediate in the cell since Zn(II) binding by the repressing CzrA-DNA complex will quickly lead to disassembly of the complex. As might be expected, qualitative inspection of the ^{1}H-^{15}N TROSY spectrum of this intermediate reveals that CzrA adopts a "hybrid" conformation as it attempts to optimize interactions with both metal and DNA ligands (A. Arunkumar and D. Giedroc, unpublished results). There are a number of residues for which backbone amide and side chain methyl chemical shifts are distinguishable in the CzrA-Zn$_2$-DNA complex relative to the apo-CzrA-DNA and allosterically inhibited Zn$_2$ states. These residues are strong candidates for playing a key role in structural coupling between metal and DNA binding sites [112], which may buttress the hydrogen bonding pathway shown (Fig, 4). In any case, when NMR studies like these are combined with a multiple sequence alignment of ArsR family regulators of known distinct metal binding sites [14, 58], this approach can be used to identify candidate residues for substitution and quantification of ΔG_c [63, 74].

6. Conformational dynamics in allosteric regulation by metals

These global thermodynamics are in general consistent with insights gleaned from residue-specific conformational dynamics, readily measured by a variety of NMR approaches. For example, the fully metallated Zn$_2$ state of CzrA, relative to apo-CzrA, reveals that Zn(II) binding rigidifies the quaternary structure of the molecule [89, 91]. The rate of hydrogen-deuterium solvent exchange of backbone amides is globally quenched [91] and investigation of the short timescale (ps-ns) dynamics and qualitative insights into intermediate (μs) timescale dynamics using the same methods are consistent with dynamical quenching of not only the α5 and α1 helical core that comprises much of the dimer interface, but also into the more peripheral α4 (DNA recognition) helices (Fig. 7). The β-hairpin is structurally unaffected, which is conformationally dynamic in both apo and metallated states [89].

This picture of the allosterically inhibited Zn$_2$ state contrasts sharply with that of repressing apo-CzrA-DNA complex relative to same apo-CzrA reference state [89]. Here, the expected stabilization of the protein-DNA interfacial region is observed; however, the metal binding sites in the α5 helix become highly mobile as evidenced by rapid H-D exchange rates and increases in backbone dynamical disorder in the *ns* to *ps* time scale, which are small but extend into the core of the protein [89]. These dynamical findings are consistent with the solution structure of the DNA-bound CzrA. This structure reveals that while the global fold of each protomer is unchanged relative to apo-CzrA, the quaternary structure differs dramatically, with the DNA recognition helices (α4) directed away from the core and pointing in a direction that allows for favorable contacts with successive major grooves of the DNA operator (see Fig. 4(a)). In order for this to occur, the α5 helices pull apart from one another and expose the core of the dimer, thus strongly enhancing conformational mobility in the allosteric sites. Enhanced dynamics in this region may well increase the kinetics of metal association and thus drive subsequent dissociation of the Zn(II)-bound repressor from the DNA [113].

Although studies of the conformational dynamics have only been reported for a few other metal sensor proteins [114, 115], functionally important stabilization of the native structure upon binding metals may be a recurring theme. This can result from metal binding to a

structural site that plays no direct role in regulation or to the regulatory site(s) directly, similar to that which occurs in CzrA. For example in *H. pylori* Fur$_{HP}$ [19, 116-120], Zn(II) binds to a tetrathiolate, distorted tetrahedral site found in a C-terminal regulatory domain involving two C-terminal Cys residues that are necessary to stabilize the dimer, but play no direct role in metalloregulation [121]. Hence, formation of this structural site is a necessary prerequisite of metal binding to the regulatory sites [121]. This S$_4$ structural site is found in many, *e.g.,* Zur [60, 88], Nur [86] and PerR [95], but not all Fur family sensors. Some Fur family dimers contain a third pair of "secondary" metal binding sites, whose coordination structure and function seems to vary from the one to another regulator [34, 40, 60, 88, 104, 122].

Similarly, DtxR/IdeR regulators often require metal occupancy of what is thought to be a secondary structural site that stabilizes the quaternary structure by increasing the stability of the dimer [70, 123-125]. This may be a necessary prerequisite for a second metal to bind to the pair of regulatory sites in the dimer [126]. In the ArsR/SmtB family, the α5 metal site that plays a regulatory role in CzrA (see Fig. 4) and in SmtB [127] is also present in many (but not all) Cd(II)/Pb(II) sensing CadCs but plays no role in regulation; it may stabilize the dimer and function as a necessary prerequisite for Cd(II) regulation in the more peripheral α3N sensing sites [128, 129]. In *E. coli* NikR, the binding of cognate metal to the C-terminal domain nucleates a hydrogen bonding network that likely stabilizes the native structure against thermal denaturation; in contrast, non-cognate metals that adopt distinct coordination structures do not [49, 52, 130]. Structural stabilization of NikR allows formation of a pair of lower affinity Ni(II) sites that are essential for full activation of *nik* operator binding [56].

The crystallographic structures of *C. diphtherium* DtxR, *M. tuberculosis* IdeR and *B. subtilis* MntR in the metal-free and allosterically activated, metal-bound states reveal only small differences that bring the pair of DNA binding domains into a more "closed" conformation which is thought to directly stabilize protein-DNA interactions [73, 126, 131-133]. An alternative interpretation of these small structural changes is that the binding of activating metals functions largely to quench conformational dynamics which "locks in" or "freezes" a high DNA-binding affinity conformation. Hydrogen-deuterium exchange mass spectrometry carried out with Mn(II)-MntR [115] and EPR spectroscopy of the structural homolog *B. anthracis* AntR [114] are generally consistent with this picture. In AntR, the DNA binding domain is characterized by an ensemble of different conformational states in rapid exchange on the *ns* timescale that are narrowed by non-cognate Zn(II) binding [114, 134]. The degree to which cognate metal Mn(II) narrows the distribution relative to Zn(II) is unknown but of interest since Zn(II) is a poor activator of operator binding by MntR and other MntR-like repressors including *S. pneumoniae* MntR and PsaR [23, 24] and *S. gordonii* ScaR [70]. A subject of ongoing work in our laboratory is to determine the degree to which allosteric inhibition and activation may possess a common origin in "stiffening" or rigidifying the metal-bound conformation [89].

7. Concluding remarks

In this review, we discuss three major emerging themes that are predicted to govern functional metal selectivity in bacterial transition metal homeostasis: *1)* Metal sensor specificity for one or a few closely related metals from different structural families seem to exhibit characteristic trends in metal affinity when measured under similar solution conditions. It is these affinities that may well govern the intracellular sensitivity of these allosteric switches in the cell, thus establishing the limits of the "buffered" concentration of metal, beyond which mediates a transcriptional response. Cu(I) and Zn(II) are highly competitive metals and thus their bioavailability is tightly controlled intracellularly by the mechanisms discussed here. *2)* Cognate metal complexes in metal sensor proteins are

characterized by a coordination geometry that optimizes subsequent noncovalent interactions that drive a structural or dynamical change in the oligomer that leads to allosteric signal propagation. This sometimes occurs through the "second" coordination shell of the inducing metal complex. *3)* Allosteric switching by metal sensor proteins involves changes in structure and/or dynamics driven by cognate metal binding and to a far lesser extent, by non-cognate metal binding. Future challenges are to determine the degree to these rules derived from a detailed analysis of only a few systems characterize other metal sensor proteins, and how nature re-engineers an existing allosteric metal site and evolves the ability to respond to other stresses, namely oxidative and nitrosative stress. How multiple parallel pathways of transition metal homeostasis and oxidative stress resistance intersect in the cell is also an important topic. Careful investigations of the quantitative biology of these fascinating allosteric proteins will continue to provide new insights into the perturbation and adaptability of the metallome in cells.

Acknowledgments

References

[1]. Berg JM, Godwin HA. Lessons from zinc-binding peptides. Annu Rev Biophys Biomol Struct. 1997; 26:357–371. [PubMed: 9241423]

[2]. Seneque O, Bonnet E, Joumas FL, Latour JM. Cooperative Metal Binding and Helical Folding in Model Peptides of Treble-Clef Zinc Fingers. Chemistry. 2009; 15:4798–4810. [PubMed: 19388025]

[3]. Auld DS. Zinc coordination sphere in biochemical zinc sites. Biometals. 2001; 14:271–313. [PubMed: 11831461]

[4]. Perry JJP, Shin DS, Getzoff ED, Tainer JA. The structural biochemistry of the superoxide dismutases. Biochim Biophys Acta. 2010; 1804:245–262. [PubMed: 19914407]

[5]. Ermler U, Grabarse W, Shima S, Goubeaud M, Thauer RK. Active sites of transition-metal enzymes with a focus on nickel. Curr Opin Struct Biol. 1998; 8:749–758. [PubMed: 9914255]

[6]. Arredondo M, Nunez MT. Iron and copper metabolism. Mol Aspects Med. 2005; 26:313–327. [PubMed: 16112186]

[7]. Singleton C, Le Brun N. Atx1-like chaperones and their cognate P-type ATPases: copper-binding and transfer. Biometals. 2007; 20:275–289. [PubMed: 17225061]

[8]. Hartwig A. Zinc Finger Proteins as Potential Targets for Toxic Metal Ions: Differential Effects on Structure and Function. Antiox Redox Signal. 2001; 3:625–634.

[9]. Valko M, Morris H, Cronin MT. Metals, toxicity and oxidative stress. Curr Med Chem. 2005; 12:1161–1208. [PubMed: 15892631]

[10]. Godwin HA. The biological chemistry of lead. Curr Opin Chem Biol. 2001; 5:223–227. [PubMed: 11282351]

[11]. Waldron KJ, Rutherford JC, Ford D, Robinson NJ. Metalloproteins and metal sensing. Nature. 2009; 460:823–830. [PubMed: 19675642]

[12]. Ma Z, Jacobsen FE, Giedroc DP. Coordination Chemistry of Bacterial Metal Transport and Sensing. Chem Rev. 2009; 109:4644–4681. [PubMed: 19788177]

[13]. Giedroc DP, Arunkumar AI. Metal sensor proteins: nature's metalloregulated allosteric switches. Dalton Trans. 2007; 7:3107–3120. [PubMed: 17637984]

[14]. Busenlehner LS, Pennella MA, Giedroc DP. The SmtB/ArsR family of metalloregulatory transcriptional repressors: Structural insights into prokaryotic metal resistance. FEMS Microbiol Rev. 2003; 27:131–143. [PubMed: 12829264]

[15]. Reyes-Caballero H, Guerra AJ, Jacobsen FE, Kazmierczak KM, Cowart D, Koppolu UMK, Scott RA, Winkler ME, Giedroc DP. The Metalloregulatory Zinc Site in *Streptococcus pneumoniae*

AdcR, a Zinc-activated MarR Family Repressor. J Mol Biol. 2010; 403:197–216. [PubMed: 20804771]

[16]. Chen H, Wu R, Xu G, Fang X, Qiu X, Guo H, Tian B, Hua Y. DR2539 is a novel DtxR-like regulator of Mn/Fe ion homeostasis and antioxidant enzyme in *Deinococcus radiodurans*. Biochem Biophys Res Comm. 2010; 396:413–418. [PubMed: 20417183]

[17]. Ernst FD, Kuipers EJ, Heijens A, Sarwari R, Stoof J, Penn CW, Kusters JG, van Vliet AHM. The Nickel-Responsive Regulator NikR Controls Activation and Repression of Gene Transcription in *Helicobacter pylori*. Infect. Immun. 2005; 73:7252–7258. [PubMed: 16239520]

[18]. Danielli A, Scarlato V. Regulatory circuits in *Helicobacter pylori* : network motifs and regulators involved in metal-dependent responses. FEMS Microbiol Rev. 2010; 34:738–752. [PubMed: 20579104]

[19]. Danielli A, Roncarati D, Delany I, Chiarini V, Rappuoli R, Scarlato V. In Vivo Dissection of the *Helicobacter pylori* Fur Regulatory Circuit by Genome-Wide Location Analysis. J Bacteriol. 2006; 188:4654–4662. [PubMed: 16788174]

[20]. Ahn B-E, Cha J, Lee E-J, Han A-R, Thompson CJ, Roe J-H. Nur, a nickel-responsive regulator of the Fur family, regulates superoxide dismutases and nickel transport in *Streptomyces coelicolor*. Mol Microbiol. 2006; 59:1848–1858. [PubMed: 16553888]

[21]. Wang S, Wu Y, Outten FW. Fur and the novel regulator YqjI control transcription of the ferric reductase gene yqjH in *Escherichia coli*. J Bacteriol. 2011; 193:563–574. [PubMed: 21097627]

[22]. Puri S, Hohle TH, O'Brian MR. Control of bacterial iron homeostasis by manganese. Proc Natl Acad Sci U S A. 2010; 107:10691–10695. [PubMed: 20498065]

[23]. Kloosterman TG, Witwicki R, Pol M, Bijlsma J, Kuipers E. Opposite effects of Mn2+ and Zn2+ on the PsaR-mediated expression of the virulence genes pcpA, prtA and psaB(CA) of *Streptococcus pneumoniae*. Mol Microbiol. 2008

[24]. Jacobsen FE, Kazmierczak KM, Lisher JP, Winkler ME, Giedroc DP. Interplay between manganese and zinc homeostasis in the human pathogen *Streptococcus pneumoniae*. Metallomics. 2011; 3:38–41. [PubMed: 21275153]

[25]. Ward SK, Abomoelak B, Hoye EA, Steinberg H, Talaat AM. CtpV: a putative copper exporter required for full virulence of *Mycobacterium tuberculosis*. Mol Microbiolbiol. 2010; 77:1096–1110.

[26]. Festa RA, Jones MB, Butler-Wu S, Sinsimer D, Gerads R, Bishai WR, Peterson SN, Darwin KH. A novel copper-responsive regulon in *Mycobacterium tuberculosis*. Mol Microbiolbiol. 2011; 79:133–148.

[27]. Wolschendorf F, Ackart D, Shrestha TB, Hascall-Dove L, Nolan S, Lamichhane G, Wang Y, Bossmann SH, Basaraba RJ, Niederweis M. Copper resistance is essential for virulence of *Mycobacterium tuberculosis*. Proc Natl Acad Sci U S A. 2011; 108:1621–1626. [PubMed: 21205886]

[28]. Outten CE, O'Halloran TV. Femtomolar Sensitivity of Metalloregulatory Proteins Controlling Zinc Homeostasis. Science. 2001; 292:2488–2492. [PubMed: 11397910]

[29]. Cavet JS, Meng W, Pennella MA, Appelhoff RJ, Giedroc DP, Robinson NJ. A nickel-cobalt-sensing ArsR-SmtB family repressor. Contributions of cytosol and effector binding sites to metal selectivity. J Biol Chem. 2002; 277:38441–38448. [PubMed: 12163508]

[30]. Chauhan S, Kumar A, Singhal A, Tyagi JS, Krishna Prasad H. CmtR, a cadmium-sensing ArsR–SmtB repressor, cooperatively interacts with multiple operator sites to autorepress its transcription in *Mycobacterium tuberculosis*. FEBS Journal. 2009; 276:3428–3439. [PubMed: 19456862]

[31]. O'Halloran TV, Frantz B, Shin MK, Ralston DM, Wright JG. The MerR heavy metal receptor mediates positive activation in a topologically novel transcription complex. Cell. 1989; 56:119–129. [PubMed: 2910495]

[32]. Outten CE, Outten FW, O'Halloran TV. DNA distortion mechanism for transcriptional activation by ZntR, a Zn(II)-responsive MerR homologue in *Escherichia coli*. J Biol Chem. 1999; 274:37517–37524. [PubMed: 10608803]

[33]. Lee PE, Demple B, Barton JK. DNA-mediated redox signaling for transcriptional activation of SoxR. Proc Natl Acad Sci U S A. 2009; 106:13164–13168. [PubMed: 19651620]

[34]. Jin-Won L, John DH. Functional specialization within the Fur family of metalloregulators. BioMetals. 2007

[35]. Patzer SI, Hantke K. The ZnuABC high-affinity zinc uptake system and its regulator Zur in *Escherichia coli*. Mol Microbiol. 1998; 28:1199–1210. [PubMed: 9680209]

[36]. Dittmer PJ, Miranda JG, Gorski JA, Palmer AE. Genetically encoded sensors to elucidate spatial distribution of cellular zinc. J Biol Chem. 2009; 284:16289–16297. [PubMed: 19363034]

[37]. Irving H, Williams RJP. Order of Stability of Metal Complexes. Nature. 1948; 162:746–747.

[38]. Panina EM, Mironov AA, Gelfand MS. Comparative genomics of bacterial zinc regulons: enhanced ion transport, pathogenesis, and rearrangement of ribosomal proteins. Proc Natl Acad Sci U S A. 2003; 100:9912–9917. [PubMed: 12904577]

[39]. Gabriel SE, Helmann JD. Contributions of Zur-Controlled Ribosomal Proteins to Growth under Zinc Starvation Conditions. J Bacteriol. 2009; 191:6116–6122. [PubMed: 19648245]

[40]. Dian C, Vitale S, Leonard GA, Bahlawane C, Fauquant C, Leduc D, Muller C, de Reuse H, Michaud-Soret I, Terradot L. The structure of the *Helicobacter pylori* ferric uptake regulator Fur reveals three functional metal binding sites. Mol Microbiolbiol. 2011; 79:1260–1275.

[41]. Robinson NJ, Winge DR. Copper Metallochaperones. Annual Review of Biochemistry. 2010; 79:537–562.

[42]. Dainty SJ, Patterson CJ, Waldron KJ, Robinson NJ. Interaction between cyanobacterial copper chaperone Atx1 and zinc homeostasis. J Biol Inorg Chem. 2009; 15:77–85. [PubMed: 19543924]

[43]. Changela A, Chen K, Xue Y, Holschen J, Outten CE, O'Halloran TV, Mondragon A. Molecular Basis of Metal-Ion Selectivity and Zeptomolar Sensitivity by CueR. Science. 2003; 301:1383–1387. [PubMed: 12958362]

[44]. Ma Z, Cowart DM, Ward BP, Arnold RJ, DiMarchi RD, Zhang L, George GN, Scott RA, Giedroc DP. Unnatural Amino Acid Substitution as a Probe of the Allosteric Coupling Pathway in a Mycobacterial Cu(I) Sensor. J Am Chem Soc. 2009; 131:18044–18045. [PubMed: 19928961]

[45]. Ma Z, Cowart DM, Scott RA, Giedroc DP. Molecular Insights into the Metal Selectivity of the Copper(I)-Sensing Repressor CsoR from Bacillus subtilis. Biochemistry. 2009; 48:3325–3334. [PubMed: 19249860]

[46]. Grossoehme N, Kehl-Fie TE, Ma Z, Adams KW, Cowart DM, Scott RA, Skaar EP, Giedroc DP. Control of copper resistance and inorganic sulfur metabolism by paralogous regulators in Staphylococcus aureus. J Biol Chem. 2011

[47]. Mills SA, Marletta MA. Metal Binding Characteristics and Role of Iron Oxidation in the Ferric Uptake Regulator from *Escherichia coli*. Biochemistry. 2005; 44:13553–13559. [PubMed: 16216078]

[48]. Chivers PT, Sauer RT. NikR repressor: High-affinity nickel binding to the C-terminal domain regulates binding to operator DNA. Chemistry & Biology. 2002; 9:1141–1148. [PubMed: 12401498]

[49]. Schreiter ER, Sintchak MD, Guo Y, Chivers PT, Sauer RT, Drennan CL. Crystal structure of the nickel-responsive transcription factor NikR. Nat Struct Mol Biol. 2003; 10:794–799.

[50]. De Pina K, Desjardin V, Mandrand-Berthelot M-A, Giordano G, Wu L-F. Isolation and Characterization of the *nikR* Gene Encoding a Nickel-Responsive Regulator in *Escherichia coli*. J Bacteriol. 1999; 181:670–674. [PubMed: 9882686]

[51]. Dosanjh NS, Michel SLJ. Microbial nickel metalloregulation: NikRs for nickel ions. Curr Opin Chem Biol. 2006; 10:123–130. [PubMed: 16504569]

[52]. Wang SC, Dias AV, Bloom SL, Zamble DB. Selectivity of metal binding and metal-induced stability of *Escherichia coli* NikR. Biochemistry. 2004; 43:10018–10028. [PubMed: 15287729]

[53]. Iwig JS, Rowe JL, Chivers PT. Nickel homeostasis in *Escherichia coli* - the *rcnR-rcnA* efflux pathway and its linkage to NikR function. Mol Microbiol. 2006; 62:252–262. [PubMed: 16956381]

[54]. Iwig JS, Leitch S, Herbst RW, Maroney MJ, Chivers PT. Ni(II) and Co(II) Sensing by *Escherichia coli* RcnR. J Am Chem Soc. 2008; 130:7592–7606. [PubMed: 18505253]
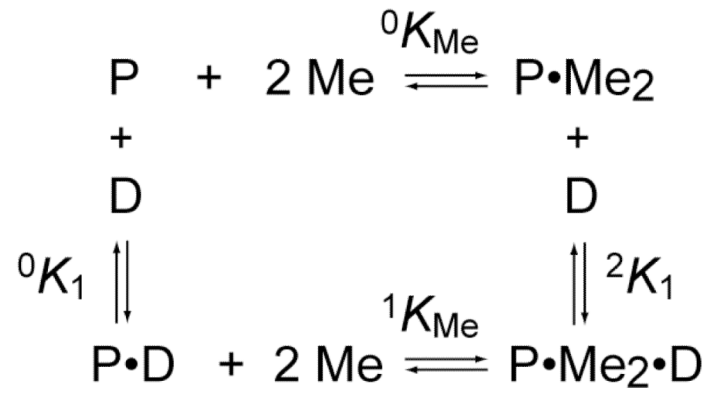
[55]. Wang SC, Dias AV, Zamble DB. The "metallo-specific" response of proteins: a perspective based on the *Escherichia coli* transcriptional regulator NikR. Dalton Trans. 2009:2459–2466. [PubMed: 19319388]

[56]. Wang SC, Li Y, Ho M, Bernal M-E, Sydor AM, Kagzi WR, Zamble DB. The Response of *Escherichia coli* NikR to Nickel: A Second Nickel-Binding Site. Biochemistry. 2010; 49:6635–6645. [PubMed: 20583753]

[57]. Osman D, Cavet JS. Bacterial metal-sensing proteins exemplified by ArsR-SmtB family repressors. Nat Prod Rep. 2010; 27:668–680. [PubMed: 20442958]

[58]. Campbell DR, Chapman KE, Waldron KJ, Tottey S, Kendall S, Cavallaro G, Andreini C, Hinds J, Stoker NG, Robinson NJ, Cavet JS. Mycobacterial cells have dual nickel-cobalt sensors: sequence relationships and metal sites of metal-responsive repressors are not congruent. J Biol Chem. 2007; 282:32298–32310. [PubMed: 17726022]

[59]. Shin JH, Oh SY, Kim SJ, Roe JH. The zinc-responsive regulator Zur controls a zinc uptake system and some ribosomal proteins in *Streptomyces coelicolor* A3(2). J Bacteriol. 2007; 189:4070–4077. [PubMed: 17416659]

[60]. Shin JH, Jung HJ, An YJ, Cho YB, Cha SS, Roe JH. Graded expression of zinc-responsive genes through two regulatory binding sites in Zur. Proc Natl Acad Sci U S A. 2011; 108 in press.

[61]. Wilkinson SP, Grove A. Ligand-responsive transcriptional regulation by members of the MarR family of winged helix proteins. Curr Issues Mol Biol. 2006; 8:51–62. [PubMed: 16450885]

[62]. Kloosterman TG, van der Kooi-Pol MM, Bijlsma JJE, Kuipers OP. The novel transcriptional regulator SczA mediates protection against Zn2+ stress by activation of the Zn2+-resistance gene czcD in *Streptococcus pneumoniae*. Mol Microbiolbiol. 2007; 65:1049–1063.

[63]. Pennella MA, Arunkumar AI, Giedroc DP. Individual Metal Ligands Play Distinct Functional Roles in the Zinc Sensor *Staphylococcus aureus* CzrA. J Mol Biol. 2006; 356:1124–1136. [PubMed: 16406068]

[64]. Golynskiy MV, Gunderson WA, Hendrich MP, Cohen SM. Metal binding studies and EPR spectroscopy of the manganese transport regulator MntR. Biochemistry. 2006; 45:15359–15372. [PubMed: 17176058]

[65]. Schmitt MP. Analysis of a DtxR-like metalloregulatory protein, MntR, from *Corynebacterium diphtheriae* that controls expression of an ABC metal transporter by an Mn2+-dependent mechanism. J Bacteriol. 2002; 184:6882–6892. [PubMed: 12446639]

[66]. Que Q, Helmann JD. Manganese homeostasis in Bacillus subtilis is regulated by MntR, a bifunctional regulator related to the diphtheria toxin repressor family of proteins. Mol Microbiol. 2000; 35:1454–1468. [PubMed: 10760146]

[67]. Glasfeld A, Guedon E, Helmann JD, Brennan RG. Structure of the manganese-bound manganese transport regulator of *Bacillus subtilis*. Nat Struct Biol. 2003; 10:652–657. [PubMed: 12847518]

[68]. Lieser SA, Davis TC, Helmann JD, Cohen SM. DNA-binding and oligomerization studies of the manganese(II) metalloregulatory protein MntR from *Bacillus subtilis*. Biochemistry. 2003; 42:12634–12642. [PubMed: 14580210]

[69]. Golynskiy MV, Davis TC, Helmann JD, Cohen SM. Metal-induced structural organization and stabilization of the metalloregulatory protein MntR. Biochemistry. 2005; 44:3380–3389. [PubMed: 15736948]

[70]. Stoll KE, Draper WE, Kliegman JI, Golynskiy MV, Brew-Appiah RAT, Phillips RK, Brown HK, Breyer WA, Jakubovics NS, Jenkinson HF, Brennan RG, Cohen SM, Glasfeld A. Characterization and Structure of the Manganese-Responsive Transcriptional Regulator ScaR. Biochemistry. 2009; 48:10308–10320. [PubMed: 19795834]

[71]. Guedon E, Helmann JD. Origins of metal ion selectivity in the DtxR/MntR family of metalloregulators. Mol Microbiol. 2003; 48:495–506. [PubMed: 12675807]

[72]. Pearson RG. Hard and soft acids and bases, HSAB, part 1: Fundamental principles. J Chem Educ. 1968; 45:581.

[73]. Kliegman JI, Griner SL, Helmann JD, Brennan RG, Glasfeld A. Structural basis for the metal-selective activation of the manganese transport regulator of *Bacillus subtilis*. Biochemistry. 2006; 45:3493–3505. [PubMed: 16533030]

[74]. Grossoehme NE, Giedroc DP. Energetics of Allosteric Negative Coupling in the Zinc Sensor *S. aureus* CzrA. J Am Chem Soc. 2009; 131:17860–17870. [PubMed: 19995076]

[75]. Pennella MA, Shokes JE, Cosper NJ, Scott RA, Giedroc DP. Structural elements of metal selectivity in metal sensor proteins. Proc Natl Acad Sci U S A. 2003; 100:3713–3718. [PubMed: 12651949]

[76]. VanZile ML, Cosper NJ, Scott RA, Giedroc DP. The zinc metalloregulatory protein *Synechococcus* PCC7942 SmtB binds a single zinc ion per monomer with high affinity in a tetrahedral coordination geometry. Biochemistry. 2000; 39:11818–11829. [PubMed: 10995250]

[77]. Maret W, Li Y. Coordination Dynamics of Zinc in Proteins. Chem Rev. 2009; 109:4682–4707. [PubMed: 19728700]

[78]. Patel K, Kumar A, Durani S. Analysis of the structural consensus of the zinc coordination centers of metalloprotein structures. Biochim Biophys Acta. 2007; 1774:1247–1253. [PubMed: 17855175]

[79]. Dudev T, Lim C. Principles governing Mg, Ca, and Zn binding and selectivity in proteins. Chem Rev. 2003; 103:773–787. [PubMed: 12630852]

[80]. Kuppuraj G, Dudev M, Lim C. Factors Governing Metal-Ligand Distances and Coordination Geometries of Metal Complexes. J Phys Chem B. 2009; 113:2952–2960. [PubMed: 19708219]

[81]. Liu T, Ramesh A, Ma Z, Ward SK, Zhang LM, George GN, Talaat AM, Sacchettini JC, Giedroc DP. CsoR is a novel *Mycobacterium tuberculosis* copper-sensing transcriptional regulator. Nat Chem Biol. 2007; 3:60–68. [PubMed: 17143269]

[82]. Chivers PT. Coordinating intracellular nickel-metal-site structure-function relationships and the NikR and RcnR repressors. Nat Prod Rep. 2010; 27:658–667. [PubMed: 20442957]

[83]. Leitch S, Bradley MJ, Rowe JL, Chivers PT, Maroney MJ. Nickel-Specific Response in the Transcriptional Regulator, *Escherichia coli* NikR. J Am Chem Soc. 2007; 129:5085–5095. [PubMed: 17397155]

[84]. Bloom SL, Zamble DB. Metal-Selective DNA-Binding Response of *Escherichia coli* NikR. Biochemistry. 2004; 43:10029–10038. [PubMed: 15287730]

[85]. Chen K, Yuldasheva S, Penner-Hahn JE, O'Halloran TV. An Atypical Linear Cu(I)-S2 Center Constitutes the High-Affinity Metal-Sensing Site in the CueR Metalloregulatory Protein. J Am Chem Soc. 2003; 125:12088–12089. [PubMed: 14518983]

[86]. An YJ, Ahn BE, Han AR, Kim HM, Chung KM, Shin JH, Cho YB, Roe JH, Cha SS. Structural basis for the specialization of Nur, a nickel-specific Fur homolog, in metal sensing and DNA recognition. Nucl Acids Res. 2009; 37:3442–3451. [PubMed: 19336416]

[87]. Ahmad R, Brandsdal BO, Michaud-Soret I, Willassen NP. Ferric uptake regulator protein: Binding free energy calculations and per-residue free energy decomposition. Proteins. 2009; 75:373–386. [PubMed: 18831042]

[88]. Lucarelli D, Russo S, Garman E, Milano A, Meyer-Klaucke W, Pohl E. Crystal Structure and Function of the Zinc Uptake Regulator FurB from *Mycobacterium tuberculosis*. J Biol Chem. 2007; 282:9914–9922. [PubMed: 17213192]

[89]. Arunkumar AI, Campanello GC, Giedroc DP. Solution structure of a paradigm ArsR family zinc sensor in the DNA-bound state. Proc Natl Acad Sci U S A. 2009; 106:18177–18182. [PubMed: 19822742]

[90]. Schreiter ER, Wang SC, Zamble DB, Drennan CL. NikR-operator complex structure and the mechanism of repressor activation by metal ions. Proc Natl Acad Sci U S A. 2006; 103:13676–13681. [PubMed: 16945905]

[91]. Eicken C, Pennella MA, Chen X, Koshlap KM, VanZile ML, Sacchettini JC, Giedroc DP. A metal-ligand-mediated intersubunit allosteric switch in related SmtB/ArsR zinc sensor proteins. J Mol Biol. 2003; 333:683–695. [PubMed: 14568530]

[92]. Arunkumar AI, Pennella MA, Kong XM, Giedroc DP. Resonance assignments of the metal sensor CzrA in the apo-, Zn2- and DNA-bound (42 kDa) states. Biomol NMR Assign. 2007; 1:99–101. [PubMed: 19636838]

[93]. Chakrabarti P. Geometry of interaction of metal-ions with histidine-residues in protein structures. Protein Engin. 1990; 4:57–63.

[94]. Alberts IL, Nadassy K, Wodak SJ. Analysis of zinc binding sites in protein crystal structures. Protein Science. 1998; 7:1700–1716. [PubMed: 10082367]

[95]. Jacquamet L, Traore DAK, Ferrer JL, Proux O, Testemale D, Hazemann JL, Nazarenko E, El Ghazouani A, Caux-Thang C, Duarte V, Latour JM. Structural characterization of the active form of PerR: insights into the metal-induced activation of PerR and Fur proteins for DNA binding. Mol Microbiol. 2009; 73:20–31. [PubMed: 19508285]

[96]. Lee J-W, Helmann JD. The PerR transcription factor senses H2O2 by metal-catalysed histidine oxidation. Nature. 2006; 440:363–367. [PubMed: 16541078]

[97]. Traoré DAK, El Ghazouani A, Ilango S, Dupuy J, Jacquamet L, Ferrer JL, Caux-Thang C, Duarte V, Latour JM. Crystal structure of the apo-PerR-Zn protein from *Bacillus subtilis*. Mol Microbiol. 2006; 61:1211–1219. [PubMed: 16925555]

[98]. Traoré DAK, Ghazouani AE, Jacquamet L, Borel F, Ferrer J-L, Lascoux D, Ravanat J-L, Jaquinod M, Blondin G, Caux-Thang C, Duarte V, Latour J-M. Structural and functional characterization of 2-oxo-histidine in oxidized PerR protein. Nat Chem Biol. 2009; 5:53–59. [PubMed: 19079268]

[99]. Won YB, Ji CJ, Cho JH, Lee JW. Mutational Analysis of the Metal-binding Sites of Peroxide Sensor PerR. Bull Kor Chem Soc. 2010; 31:1573–1576.

[100]. Giedroc DP. Hydrogen peroxide sensing in *Bacillus subtilis* : it is all about the (metallo)regulator. Mol Microbiol. 2009; 73:1–4. [PubMed: 19508286]

[101]. Lee JW, Helmann JD. Functional specialization within the Fur family of metalloregulators. Biometals. 2007; 20:485–499. [PubMed: 17216355]

[102]. Lucarelli D, Vasil ML, Meyer-Klaucke W, Pohl E. The metal-dependent regulators FurA and FurB from *Mycobacterium tuberculosis*. Internat J Mol Sci. 2008; 9:1548–1560.

[103]. Pohl E, Haller JC, Mijovilovich A, Meyer-Klaucke W, Garman E, Vasil ML. Architecture of a protein central to iron homeostasis: crystal structure and spectroscopic analysis of the ferric uptake regulator. Mol Microbiol. 2003; 47:903–915. [PubMed: 12581348]

[104]. Sheikh A, Taylor GL. Crystal structure of the *Vibrio cholerae* ferric uptake regulator (Fur) reveals insights into metal co-ordination. Mol Microbiol. 2009; 72:1208–1220. [PubMed: 19400801]

[105]. Changela A, Chen K, Xue Y, Holschen J, Outten C, O'Halloran T, Mondragon A. Molecular Basis of Metal-Ion Selectivity and Zeptomolar Sensitivity by CueR. Science. 2003; 301:1383–1387. [PubMed: 12958362]

[106]. Kern D, Zuiderweg ER. The role of dynamics in allosteric regulation. Curr Opin Struct Biol. 2003; 13:748–757. [PubMed: 14675554]

[107]. Popovych N, Sun S, Ebright RH, Kalodimos CG. Dynamically driven protein allostery. Nat Struct Mol Biol. 2006; 13:831–838. [PubMed: 16906160]

[108]. Tsai C-J, del Sol A, Nussinov R. Allostery: Absence of a Change in Shape Does Not Imply that Allostery Is Not at Play. J Mol Biol. 2008; 378:1–11. [PubMed: 18353365]

[109]. Zotin AI. Thermodynamic aspects of developmental biology. Mono Dev Biol. 1972; 5:i–viii. 1–159.

[110]. Reinhart GD. Quantitative analysis and interpretation of allosteric behavior. Methods Enzymol. 2004; 380:187–203. [PubMed: 15051338]

[111]. Lee S, Arunkumar AI, Chen X, Giedroc DP. Structural Insights into Homo- and Heterotropic Allosteric Coupling in the Zinc Sensor *S. aureus* CzrA from Covalently Fused Dimers. J Am Chem Soc. 2006; 128:1937–1947. [PubMed: 16464095]

[112]. Fenton AW. Allostery: an illustrated definition for the 'second secret of life'. Trends Biochem Sci. 2008; 33:420–425. [PubMed: 18706817]

[113]. Hilser VJ, Thompson EB. Intrinsic disorder as a mechanism to optimize allosteric coupling in proteins. Proc Natl Acad Sci U S A. 2007; 104:8311–8315. [PubMed: 17494761]

[114]. Sen KI, Logan TM, Fajer PG. Protein dynamics and monomer-monomer interactions in AntR activation by electron paramagnetic resonance and double electron-electron resonance. Biochemistry. 2007; 46:11639–11649. [PubMed: 17880108]

[115]. Golynskiy M, Li S, Woods VL Jr. Cohen SM. Conformational studies of the manganese transport regulator (MntR) from *Bacillus subtilis* using deuterium exchange mass spectrometry. J Biol Inorg Chem. 2007; 12:699–709. [PubMed: 17342524]

[116]. Delany I, Spohn G, Rappuoli R, Scarlato V. The Fur repressor controls transcription of iron-activated and -repressed genes in *Helicobacter pylori*. Mol Microbiolbiol. 2001; 42:1297–1309.

[117]. Delany I, Pacheco ABF, Spohn G, Rappuoli R, Scarlato V. Iron-Dependent Transcription of the *frpB* Gene of *Helicobacter pylori* Is Controlled by the Fur Repressor Protein. J Bacteriol. 2001; 183:4932–4937. [PubMed: 11466300]

[118]. Harris AG, Hinds FE, Beckhouse AG, Kolesnikow T, Hazell SL. Resistance to hydrogen peroxide in *Helicobacter pylori*: role of catalase (KatA) and Fur, and functional analysis of a novel gene product designated 'KatA-associated protein', KapA (HP0874). Microbiology. 2002; 148:3813–3825. [PubMed: 12480885]

[119]. Ernst FD, Bereswill S, Waidner B, Stoof J, Mader U, Kusters JG, Kuipers EJ, Kist M, van Vliet AHM, Homuth G. Transcriptional profiling of *Helicobacter pylori* Fur- and iron-regulated gene expression. Microbiology. 2005; 151:533–546. [PubMed: 15699202]

[120]. Ernst FD, Homuth G, Stoof J, Mader U, Waidner B, Kuipers EJ, Kist M, Kusters JG, Bereswill S, van Vliet AHM. Iron-Responsive Regulation of the *Helicobacter pylori* Iron-Cofactored Superoxide Dismutase SodB Is Mediated by Fur. J. Bacteriol. 2005; 187:3687–3692. [PubMed: 15901691]

[121]. Vitale S, Fauquant C, Lascoux D, Schauer K, Saint-Pierre C, Michaud-Soret I. A ZnS4 Structural Zinc Site in the *Helicobacter pylori* Ferric Uptake Regulator. Biochemistry. 2009; 48:5582–5591. [PubMed: 19419176]

[122]. Carpenter BM, Gancz H, Benoit SL, Evans S, Olsen CH, Michel SLJ, Maier RJ, Merrell DS. Mutagenesis of Conserved Amino Acids of *Helicobacter pylori* Fur Reveals Residues Important for Function. J. Bacteriol. 2010; 192:5037–5052. [PubMed: 20644138]

[123]. Tao X, Zeng HY, Murphy JR. Transition metal ion activation of DNA binding by the diphtheria tox repressor requires the formation of stable homodimers. Proc Natl Acad Sci U S A. 1995; 92:6803–6807. [PubMed: 7624323]

[124]. Spiering MM, Ringe D, Murphy JR, Marletta MA. Metal stoichiometry and functional studies of the diphtheria toxin repressor. Proc Natl Acad Sci U S A. 2003; 100:3808–3813. [PubMed: 12655054]

[125]. Love JF, vanderSpek JC, Marin V, Guerrero L, Logan TM, Murphy JR. Genetic and biophysical studies of diphtheria toxin repressor (DtxR) and the hyperactive mutant DtxR(E175K) support a multistep model of activation. Proc Natl Acad Sci U S A. 2004; 101:2506–2511. [PubMed: 14983039]

[126]. D'Aquino JA, Tetenbaum-Novatt J, White A, Berkovitch F, Ringe D. Mechanism of metal ion activation of the diphtheria toxin repressor DtxR. Proc Natl Acad Sci U S A. 2005; 102:18408–18413. [PubMed: 16352732]

[127]. VanZile ML, Chen X, Giedroc DP. Structural characterization of distinct α3N and α5 metal sites in the cyanobacterial zinc sensor SmtB. Biochemistry. 2002; 41:9765–9775. [PubMed: 12146942]

[128]. Kandegedara A, Thiyagarajan S, Kondapalli KC, Stemmler TL, Rosen BP. Role of Bound Zn(II) in the CadC Cd(II)/Pb(II)/Zn(II)-responsive Repressor. J Biol Chem. 2009; 284:14958–14965. [PubMed: 19286656]

[129]. Busenlehner LS, Weng TC, Penner-Hahn JE, Giedroc DP. Elucidation of primary (α3N) and vestigial (α5) heavy metal-binding sites in *Staphylococcus aureus* pI258 CadC: Evolutionary implications for metal ion selectivity of ArsR/SmtB metal sensor proteins. J Mol Biol. 2002; 319:685–701. [PubMed: 12054863]

[130]. Phillips CM, Schreiter ER, Guo Y, Wang SC, Zamble DB, Drennan CL. Structural basis of the metal specificity for nickel regulatory protein NikR. Biochemistry. 2008; 47:1938–1946. [PubMed: 18193897]

[131]. DeWitt MA, Kliegman JI, Helmann JD, Brennan RG, Farrens DL, Glasfeld A. The conformations of the manganese transport regulator of *Bacillus subtilis* in its metal-free state. J Mol Biol. 2007; 365:1257–1265. [PubMed: 17118401]

[132]. Tanaka T, Shinkai A, Bessho Y, Kumarevel T, Yokoyama S. Crystal structure of the manganese transport regulatory protein from *Escherichia coli*. Proteins. 2009; 77:741–746. [PubMed: 19701940]

[133]. Wisedchaisri G, Chou CJ, Wu MT, Roach C, Rice AE, Holmes RK, Beeson C, Hol WGJ. Crystal structures, metal activation, and DNA-binding properties of two-domain IdeR from *Mycobacterium tuberculosis*. Biochemistry. 2007; 46:436–447. [PubMed: 17209554]

[134]. Sen KI, Sienkiewicz A, Love JF, vanderSpek JC, Fajer PG, Logan TM. Mn(II) binding by the anthracis repressor from *Bacillus anthracis*. Biochemistry. 2006; 45:4295–4303. [PubMed: 16566604]

[135]. Liu T, Golden JW, Giedroc DP. A zinc(II)/lead(II)/cadmium(II)-inducible operon from the Cyanobacterium anabaena is regulated by AztR, an α3N ArsR/SmtB metalloregulator. Biochemistry. 2005; 44:8673–8683. [PubMed: 15952774]

[136]. Liu T, Chen XH, Ma Z, Shokes J, Hemmingsen L, Scott RA, Giedroc DP. A Cu-I-sensing ArsR family metal sensor protein with a relaxed metal selectivity profile. Biochemistry. 2008; 47:10564–10575. [PubMed: 18795800]

[137]. Jian X, Wasinger EC, Lockard JV, Chen LX, He C. Highly Sensitive and Selective Gold(I) Recognition by a Metalloregulator in *Ralstonia metallidurans*. J Am Chem Soc. 2009; 131:10869–10871. [PubMed: 19606897]

[138]. Li YJ, Zamble DB. pH-Responsive DNA-Binding Activity of *Helicobacter pylori* NikR. Biochemistry. 2009; 48:2486–2496. [PubMed: 19170600]

[139]. Rowe JL, Starnes GL, Chivers PT. Complex Transcriptional Control Links NikABCDE-Dependent Nickel Transport with Hydrogenase Expression in *Escherichia coli*. J Bacteriol. 2005; 187:6317–6323. [PubMed: 16159764]

[140]. DeLano, WL. The PyMol molecular graphics system, Version 1.2r3pre. Schrödinger; LLC, San Carlos: 2004.

$$P + 2\,Me \underset{}{\overset{^0K_{Me}}{\rightleftharpoons}} P{\cdot}Me_2$$

$$+ \qquad\qquad +$$

$$D \qquad\qquad D$$

$$^0K_1 \updownarrow \qquad \overset{^1K_{Me}}{\qquad} \qquad \updownarrow\, ^2K_1$$

$$P{\cdot}D + 2\,Me \underset{}{\overset{^1K_{Me}}{\rightleftharpoons}} P{\cdot}Me_2{\cdot}D$$

$$\Delta G_c = -RT\ln(^1K_{Me}/^0K_{Me}) = -RT\ln(^2K_1/^0K_1)$$

Figure 1.
A coupled equilibrium thermodynamic scheme that defines the relationship of all four allosteric states of the homodimer repressor (P) in equilibrium with DNA operator (D) and metal ions (Me), with a limiting stoichiometry of two metals per dimer. The allosteric coupling free energy, ΔG_c, is defined as indicated.
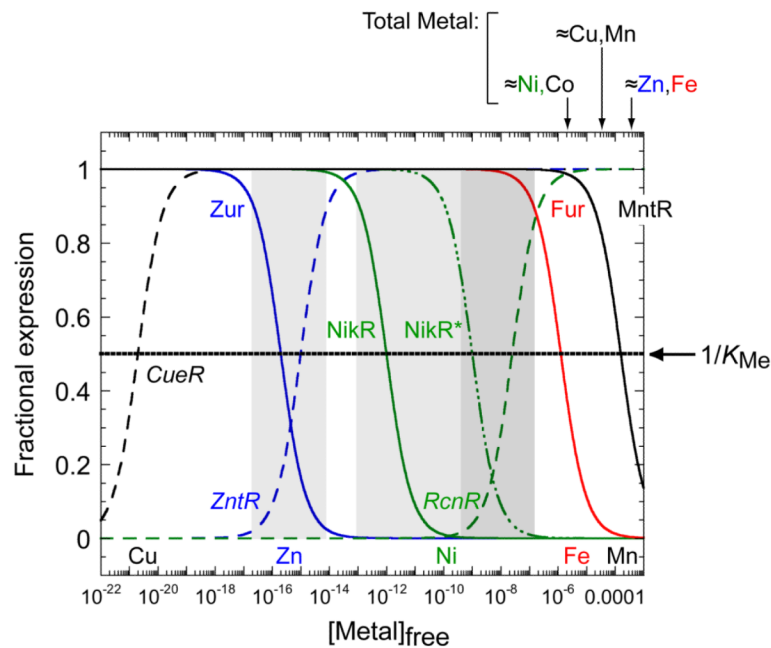
Figure 2.
A graphical representation of the hypothesis that metal affinity for individual or pairs of metal sensor proteins ($1/K_{Me}$) defines the ability of the cytoplasm to buffer biologically required transitions metal ions. Cu(I), *black*; Zn(II), *blue*; Ni(II), *green*; Fe(II), *red*; Mn(II), *black*. See Table 1 for K_{Me} values for the regulators indicated. Efflux regulators are *italicized*, with transcriptional response curves (derepression or activation) represented by the *dashed* lines; uptake repressors are in *straight* font and transcriptional response curves (corepression) represented by the *solid* lines. NikR* represents filling of the secondary, low affinity sites which give rise to full repression of the high affinity nickel uptake system [48]. Approximate total cell-associated concentrations measured in *E. coli* under aerobic growth conditions on a minimal media are shown above the figure [28]; recent studies suggest that these concentrations are ≈5-fold larger in *S. pneumoniae*, which also exhibits a high Mn(II) quota relative to Fe(II) [24]. Note that this model is predicated on the simple notion that metal sensors are capable of "scanning" the cytoplasm for metal; this may not be the case [29, 139].
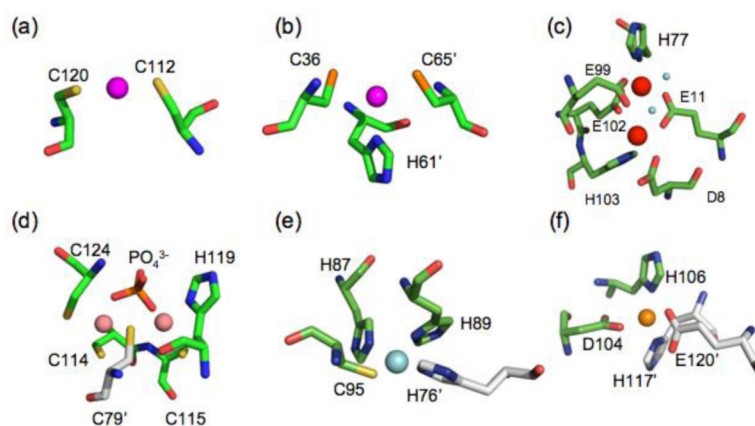
Figure 3.
Native metal coordination geometries for selected bacterial metalloregulatory proteins. A *colored* sphere represent the metal ion unless is otherwise indicated. (a) *E. coli* CueR, Cu(I) linear (PDB ID:1Q05), (b) *M. tuberculosis* CsoR, trigonal Cu(I) (PDB ID: 2HH7), (c) *B. subtilis* MntR, penta-coordinate dinuclear Mn(II), H_2O molecules are represented as cyan spheres (PDB ID: 1ON1), (d) *E. coli* ZntR, tetrahedral dinuclear Zn(II) (PDB ID: 1Q08), (e) *E. coli* NikR, square planar Ni(II) (PDB ID: 2HZV), (f) *S. elongatus* PC7942 SmtB, Zn(II) tetrahedral (PDB ID: 1R22). Graphical representation was created using PyMol [140].
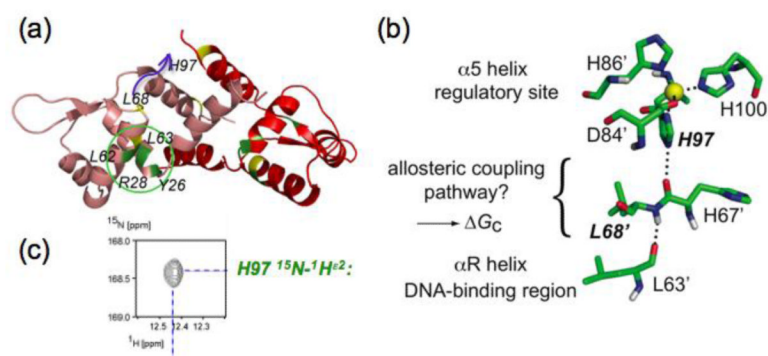
Figure 4.
Illustration of a potential hydrogen bonding pathway in CzrA that links the metal binding and DNA binding sites. (a) Ribbon representation of the solution structure of CzrA bound to DNA with key residues highlighted [89] The *blue arrow* defines the distance (≈ 10 Å) between the L68′ and H97 on opposite protomers that are proposed to hydrogen bond in the allosterically inhibited Zn_2-bound state (see panel b). (b) Two hydrogen bonds are proposed to link the $NH^{\varepsilon 2}$ of His97 with the main chain C=O of L63′ in the DNA binding αR helix [91]. (c) ^{15}N-^1H correlation for the $HN^{\varepsilon 2}$ group of H97 observed in a simple ^{15}N-^1H HSQC spectrum of Zn_2-CzrA, indicative of slow exchange with solvent in the allosterically inhibited metal-bound state, consistent with a hydrogen bonding interaction. This correlation is found in all first coordination shell mutants of CzrA that are capable of negatively regulating DNA binding upon Zn(II) binding [63], and is lost in apo-CzrA [91].
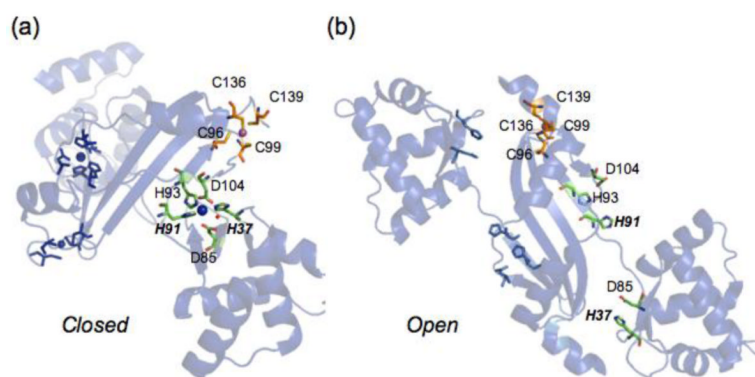
Figure 5.
The first coordination shell of a liganding histidine as an allosteric trigger in moving from the (a) "closed" PerRMnZn (3F89) and (b) "open" apo-Zn (2FE3) structures. The structure shows two metal binding sites occupied by Mn(II) (blue) and Zn(II) (magenta). Mn(II) binds to the regulatory site in a distorted square pyramidal geometry involving ligands H37 and H91 and in the Fe(II) complex, an open coordination site that accommodate H_2O_2. Zn(II) binds to a thiolate rich site that plays no role in the catalysis [95, 96], but is essential for structural integrity of the dimer [99].
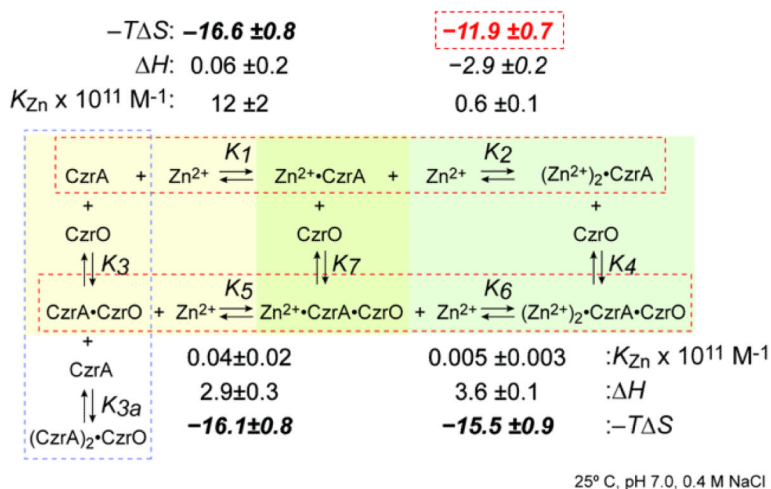
Figure 6.
Global energetics of the step-wise coupled equilibrium that describes the allosteric effect of Zn(II) binding to CzrA free in solution and when bound to DNA. Thermodynamic parameters determined by isothermal titration calorimetry (ITC) are shown [74] at pH 7.0, 0.4 M NaCl. 25.0 °C.. This is an expanded thermodynamic linkage scheme relative to that outlined in Fig. 1. CzrO, *czr* DNA operator. K_1, K_2, K_5 and K_6 are K_{Zn}^i from each step in the equilbrium where $\Delta G_i = -RT \ln K_{Zn}^i$. Allosteric (heterotropic) coupling free energies, ΔG_c^i are obtained as follows: $\Delta G_c^1 = \Delta G_5 - \Delta G_1$ (defined by the *yellow* box); $\Delta G_c^2 = \Delta G_6 - \Delta G_2$ (defined by the *green* box); $\Delta G_c^t = (\Delta G_5 + \Delta G_6) - (\Delta G_1 + \Delta G_2) = \Delta G_c^1 + \Delta G_c^2 = \Delta G_4 - \Delta G_3$ (overall linkage). See text for other details.
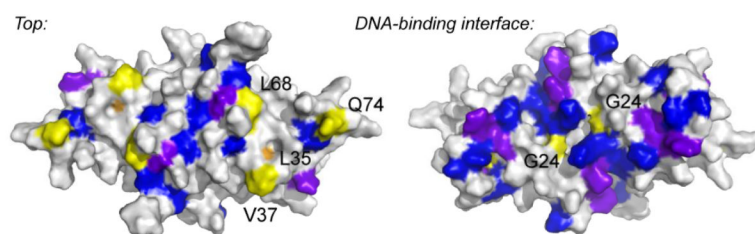
Figure 7.
Zinc binds to apo-CzrA homodimer and quenches the conformational dynamics in the core α5, α1 helical regions but also in more peripheral DNA-binding αR helices of the molecule [89]. Spacefilling models of Zn$_2$ CzrA are shown (*left*, α5 helices on top; *right*, view from the DNA-binding interface) with residues shaded according to a specific change in dynamics relative to apo-CzrA. *Blue*, residues for which the order parameter S^2 increases (≥0.02); *purple*, residues for which significant chemical exchange broadening (R_{ex}) is lost on Zn(II) binding; *beige*, residues for which R_{ex} becomes measurable upon Zn(II) binding; *yellow*, residues for which S^2 decreases on Zn(II) binding. This picture is consistent with significant quenching of the conformational dynamics (indicated by *blue, purple* residues) far from the allosteric zinc binding sites, relative to those residues which increase their motional disorder (*beige, yellow*); these may define "hinge" regions in the allosterically inhibited Zn(II) conformational ensemble [90].

Table 1

Metal binding affinities (K_{Me}) for selected bacterial transition metal sensor proteins

Regulator	Biological Process[a]	Cognate metal	Family	Species	Metal	log K_{Me}	pH	Reference
Zur	uptake	Zn	Fur	*E. coli*	**Zn(II)**	**15.7**	7.6	[28]
ZntR	efflux	Zn	MerR	*E. coli*	**Zn(II)**	**15.0**	7.6	[28]
CzrA	efflux	Zn	ArsR	*S. aureus*	**Zn(II)**	**12.4** [b]	7.0	[63]
					Co(II)	9.0	7.0	
SmtB	efflux/seq'n	Zn	ArsR	*Synechococcus*	**Zn(II)**	**11.3** [c]	7.4	[127]
					Co(II)	9.7	7.4	
AztR	efflux/seq'n	Zn/Cd	ArsR	*Anabaena PCC7120*	**Zn(II)**	**>10**	7.0	[135]
					Co(II)	≥7.3	7.0	
					Cd(II)	7.3	7.0	
					Pb(II)	6.2	7.0	
BxmR	efflux/seq'n	Zn/Cd/Cu/Ag	ArsR	*O. brevis*	**Zn(II)**	**13.0** [d]	6.3	[136]
					Cu(I)	**7.6** [e]	6.3	
AdcR	uptake	Zn	MarR	*S. pneumoniae*	**Zn(II)**	**12.1** [f] **10.0** [f]	8.0 6.0	[15]
					Co(II)	6.8 5.4	8.0 6.0	
					Mn(II)	5.1	8.0	
CueR	efflux	Cu	MerR	*E. coli*	**Cu(I)**	**20.7**	8.0	[43, 137]
					Au(I)	34.7	7.7	
CsoR_BS	efflux	Cu	CsoR	*B. subtilis*	Zn(II)	8.2	6.5	[45]
					Cu(I)	**≥19.0**	6.5	
					Ni(II)	9.5	6.5	
					Co(II)	≤5.0	6.5	
CsoR_MT	efflux	Cu		*M. tuberculosis*	**Cu(I)**	**18.0**	7.0	[44]
CsoR_SA	efflux	Cu		*S. aureus*	**Cu(I)**	**18.1**	7.0	[46]
CupR	efflux	Au	MerR	*R. metallidurans*	**Au(I)**	**34.1**	7.7	[137]

Regulator	Biological Process[a]	Cognate metal	Family	Species	Metal	log K_{Me}	pH	Reference
NikR$_{EC}$	uptake	Ni	NikR	E. coli	Cu(I)	16.1, 18.2	7.7	
					Zn(II)	>12.0	7.6	[52]
					Cu(II)	16.9	7.6	
					Ni(II)	**12.0**	7.6	
					Co(II)	8.7	7.6	
					Cd(II)	>9.0	7.6	
NikR$_{HP}$	uptake	Ni	NikR	H. pylori	**Ni(II)**	**11.5** **8.8**	7.6 5.8	[138]
NmtR	efflux	Ni/Co	ArsR	M. tuberculosis	Zn(II)	≥9.0	7.0	[29]
					Ni(II)	**10.0**	7.0	footnote g
					Co(II)	**5.9**	7.0	[29]
RcnR	efflux	Ni/Co	CsoR	E. coli	**Ni(II)**	**>7.6**	7.0	[54]
					Co(II)	**>8.3**	7.0	
Fur	uptake	Fe	Fur	E. coli	Zn(II)	5.9	7.0	[47]
					Co(II)	6.8	7.0	
					Fe(II)	**5.9**	7.0	
					Mn(II)	4.6	7.0	
MntR	uptake	Mn	DtxR	B. subtilis	Zn(II)	7.9	7.2	[64]
					Ni(II)	5.7	7.2	
					Co(II)	5.3	7.2	
					Mn(II)	**3.8** ^{h}	7.2	
					Cd(II)	**7.0**	7.2	

B. anthracis AntR (an MntR homolog), log K_{Mn}=4.2 determined using EPR spectroscopy [134].

[a] Indicated regulator controls the transcription of genes encoding proteins involved in metal uptake into the cytoplasm (uptake), extrusion from the cytoplasm (efflux), and of intracellular sequestration by metallothionens (seq'n).

[b] First of two binding sites (K_{Zn}1) on the dimer (see text for details).

[c] α5 site affinity.

[d] α5 site affinity.

[e]α3N site average affinity for each of two bound Cu(I) ions bound in a Cu2 cluster.

[f]Highest affinity regulatory site; lower affinity sites not shown.

[g]H. Reyes-Caballero, D. Giedroc, manuscript in preparation.

[h]Determined by EPR spectroscopy.